

## Preparation and application of tectoridin-imprinted magnetite nanoparticles

Yujin Pan, Qiuyan Zhang, Zhenzhen Li, Qing Wang, Changjing Ren, Sai Li, Hui Li, Qiang Zhao

College of Chemical Engineering, Sichuan University, Chengdu Sichuan, 610065, China

Y. Pan and Q. Zhang—co-first authors.

Correspondence to: Q. Zhao (E-mail: Zhaoqiang@scu.edu.cn)

**ABSTRACT:** In this work, the tectoridin-imprinted magnetite nanoparticles (TIMNPs) were firstly prepared by using tectoridin as template molecule, methacrylic acid as functional monomer, styrene as crosslinking agent, and superparamagnetic Fe<sub>3</sub>O<sub>4</sub> particles as magnetic component. TIMNPs with a size of about 161 nm were characterized by scanning electron microscope (SEM), transmission electron microscope (TEM), Fourier transform infrared (FT-IR), X-ray diffraction (XRD), vibrating sample magnetometer (VSM), and thermogravimetric analysis (TGA). Rebinding experiments were carried out to determine the specific binding properties and adsorption selectivity. The maximum number of binding sites was 69.58 μmol/g and there was only one kind of binding sites existed in TIMNPs. The relative separation factors for tectoridin with its analogues such as baicalin and atenolol were 2.63 and 2.66, respectively. The results indicated that the synthesized TIMNPs had excellent saturation magnetization, binding capacity, and adsorption selectivity. TIMNPs could be one of the most promising candidates for tectoridin extraction. © 2016 Wiley Periodicals, Inc. *J. Appl. Polym. Sci.* 2016, 133, 43806.

**KEYWORDS:** adsorption; magnetism and magnetic properties; molecular recognition; nanoparticles, nanowires and nanocrystals; separation techniques

Received 15 December 2015; accepted 15 April 2016

DOI: 10.1002/app.43806

### INTRODUCTION

*Iris tectorum Maxim*, a very popular Chinese traditional medicine, is usually used for treatment of inflammation, asthma and other throat disorders, such as cough, tonsillitis and pharyngitis.<sup>1</sup> It has been found to have inhibiting effect toward *Pseudomonas aeruginosa*, *Gonococcus*, *Pneumococcus*, and *Mycobacterium tuberculosis*.<sup>2</sup> More recently, it has been used to fight against severe acute respiratory syndrome (SARS) due to its antiviral activity.<sup>3</sup> Tectoridin, a major isoflavone found in the *I. tectorum*, exhibited estrogenic activity,<sup>4</sup> hypoglycemic action,<sup>5</sup> anti-oxidation,<sup>6</sup> anti-inflammatory,<sup>7</sup> and anti-tumor activity.<sup>8</sup> It is often used for the quality control of *I. tectorum*. Tectoridin is usually separated by macroporous resin.<sup>9,10</sup> This conventional extraction of tectoridin is time-consuming, laborious, and expensive strategy, and sometimes leads to the activities decrease during the isolation and purification process.<sup>11</sup> Therefore, a more efficient approach is expected for extracting tectoridin from *I. tectorum*.

In more recent years, molecularly imprinted polymers (MIPs) have aroused extensive research interest. MIPs are prepared by copolymerizing functional monomers and crosslinking agent around the template. With the advantages of predetermination, specific recognition and broad applicability, MIPs have become a sort of powerful tool

used for certain fields, such as separation processes<sup>12–15</sup> (chromatography, solid-phase extraction, and membrane separation), immunoassay,<sup>16</sup> sensor,<sup>17,18</sup> catalysis,<sup>19,20</sup> and artificial enzyme.<sup>21,22</sup>

The MIPs have some drawbacks still, such as heterogeneous distribution of the imprinting sites, low binding capacity, and slow binding kinetics. The nanosized particles with high surface-to-volume ratio are introduced<sup>23–26</sup> to improve the removal of template molecules, binding capacity, and binding kinetics. After extraction, the MIPs leave complementary cavities behind<sup>27,28</sup> which improve the binding capacity compared with non-imprinted polymers (NIPs). Haupt *et al.* demonstrated for the first time that water-compatible MIP particles with size of below 500 nm could be used as specific enzyme inhibitors.<sup>29,30</sup> Abdin *et al.* successfully synthesized endotoxin-MIP nanoparticles with high affinity toward endotoxin and the particle size was about 190 – 220 nm with low polydispersity index.<sup>31</sup>

Magnetic separation technology has received considerable attention due to the high magnetic susceptibility which is especially useful for a rapid and simple separation and large-scale operation. Magnetic molecularly imprinted polymers (MMIPs) binding target molecules can be easily collected and separated by an external magnetic field without additional centrifugation or filtration.<sup>32</sup> Moreover, MMIPs,

prepared by coating magnetic nanoparticles (MNPs) with MIPs, can not only selectively recognize the template molecules in the solution, but also process more imprinted cavities within the polymer network because of high surface-to-volume ratio of MNPs.<sup>33</sup> Li *et al.* successfully synthesized the core-shell bovine hemoglobin (BHb) imprinted MNPs with a mean diameter of 210 nm.<sup>34</sup> The imprinted magnetic nanoparticles could reach the adsorption equilibrium within 80 minutes and be separated quickly by an external magnetic field. Xin *et al.* had synthesized estrone-imprinted MNPs which exhibited a much higher specific recognition in estrone separation.<sup>35</sup> Niu *et al.* had synthesized MMIPs with a high recognition ability and fast binding kinetics for selective recognition of 3-methylindole.<sup>28</sup> In this article, we combined MIPs with MNPs to get nanosized MMIPs for tectoridin extraction. The synthesized TIMNPs exhibited good properties of both MIPs and MNPs. They dispersed well in solution and could be separated quickly by an external magnetic field. These properties make TIMNPs one of the most promising candidates for tectoridin extraction.

## EXPERIMENTAL

### Materials

Ferric trichloride hexahydrate ( $\text{FeCl}_3 \cdot 6\text{H}_2\text{O}$ ), ferrous chloride tetrahydrate ( $\text{FeCl}_2 \cdot 4\text{H}_2\text{O}$ ) and ammonium hydroxide (28–30%  $\text{NH}_3 \cdot \text{H}_2\text{O}$ ), 2,2-azobisisobutyronitrile (AIBN), cyclohexane (99%), sodium dodecylbenzenesulfonate (SDBS), and methacrylic acid (MAA), were purchased from Chengdu Kelong Chemical Reagent Company (People's Republic of China) and used as received.

Styrene from Chengdu Kelong Chemical Reagent Company (People's Republic of China) was washed by 5% NaOH and redistilled water in turns to remove the polymerization inhibitor.

Tectoridin is kindly gifted by Prof. Hui Li of Sichuan University.

Water used in the experiments was redistilled water.

### Synthesis of Hydrophobized Magnetite Nanoparticles (MNPs)

$\text{Fe}_3\text{O}_4$  magnetic nanoparticles were prepared by a co-precipitation method.  $\text{FeCl}_3 \cdot 6\text{H}_2\text{O}$  and  $\text{FeCl}_2 \cdot 4\text{H}_2\text{O}$  (ratio 3:2) were dissolved in 100 mL water and added into a 500 mL three-necked flask. Then ammonium hydroxide (28–30%  $\text{NH}_3 \cdot \text{H}_2\text{O}$ ) was slowly added into the solution with rapid stirring until pH 11 under nitrogen. The solution was heated to 60 °C for 3 h and then increased the temperature to 90 °C for 1 h to remove the excess ammonia. The products were washed by ethanol and water in turns for several times and then dried under vacuum.

### Preparation of TIMNPs

TIMNPs were synthesized by an improved method reported by Hui-Ying Wen *et al.*<sup>36</sup> using miniemulsion polymerization. Figure 1 shows the synthesis procedure of TIMNPs.

About 0.1 mmol tectoridin and 1 mmol MAA were mixed under sonication and pre-assembled for 12 h. About 0.1 g  $\text{Fe}_3\text{O}_4$  magnetic nanoparticles were dispersed in water for further use. The pre-assembly solution and 0.35 g co-emulsifier hexadecane were dissolved in 0.03 mmol styrene to form the oil phase. 0.175 g SDBS was dissolved in 100 mL water as the aqueous phase. Then the two phases were subjected to sonication for 30 min to get a homogeneous emulsion. The  $\text{Fe}_3\text{O}_4$  disper-

sion was added in the emulsion followed by another ultrasonication process for 15 min. All the reactants were removed into a 150 mL three-necked round-bottom flask and then added 0.03 mmol AIBN to initiate reaction. The polymerization was carried out under nitrogen atmosphere with a mechanical stirring at 300 rpm. The reaction was kept at 70 °C for 24 h.

The resulting particles were washed with methanol and acetic acid (4:1, V/V) for several times until the template molecule could not be detected by UV analysis. The particles were then washed with water and methanol in turns for three times and dried at 50 °C under vacuum.

The non-imprinted magnetite nanoparticles (NIMNPs) were prepared and treated in the same manner without tectoridin.

### Binding Experiments

The binding properties of TIMNPs were investigated by isothermal batch static equilibrium adsorption. TIMNPs (100 mg) were placed in a 25 mL conical flask and mixed with 10 mL of tectoridin solution with specific initial concentrations ranging from 0.2 to 2.5 mmol/L. After shaken at 30 °C for 24 h, TIMNPs were separated by an external magnetic field. The free concentration of tectoridin was diluted by ethanol-water solvent (70%) and measured by UV-vis spectrophotometry at 265.5 nm. In addition, the amount of tectoridin adsorbed to NIMNPs was also determined in parallel.

## RESULTS AND DISCUSSION

### Characterization

Scanning electron microscope (SEM) image (Figure 2) showed that the obtained TIMNPs with a size of about 161 nm (measured by Nano measurer software) were quasi-spherical. TIMNPs with high specific surface area and high surface activity could adsorb ions or molecules in the solution which is benefit to their binding ability.<sup>37</sup>

Transmission electron microscope (TEM) image of TIMNPs is provided in Figure 3. The size of TIMNPs is about 155 nm with spherical morphology which matches well with the result of SEM image. It is obvious that  $\text{Fe}_3\text{O}_4$  particles were entrapped in TIMNPs, indicating that TIMNPs can be separated by magnetic field quickly.

The infrared spectra of the  $\text{Fe}_3\text{O}_4$  (a) and TIMNPs (b) were measured by Nicolet NEXUS-670 FTIR apparatus (The United States) and shown in Figure 4. The absorption bands around  $560 \text{ cm}^{-1}$  of TIMNPs correspond to the Fe—O bond of  $\text{Fe}_3\text{O}_4$  particles. Absorption bands at 3421.15 and  $1635.37 \text{ cm}^{-1}$  in  $\text{Fe}_3\text{O}_4$  belong to the vibration of remaining  $\text{H}_2\text{O}$  in the samples. TIMNPs have got some new peaks, absorption bands at 3023.88, 2915.89, and  $1446.37 \text{ cm}^{-1}$  are characteristic absorption peaks of  $-\text{CH}_2$  due to the stretching vibration of polystyrene. Peaks at 1598.72 and  $1488.80 \text{ cm}^{-1}$  are attributed to the in-plane stretching of benzene ring<sup>38</sup> and the double peak of 754.04 and  $698.12 \text{ cm}^{-1}$  are the characteristic bands of polystyrene. The results confirm that the  $\text{Fe}_3\text{O}_4$  nanoparticles are combined with polystyrene.

Figure 5 shows XRD patterns of  $\text{Fe}_3\text{O}_4$  nanoparticles and TIMNPs. The relative intensity and main peaks in the  $2\theta$  ranging from 20 to 70° are quite similar to those of synthesized

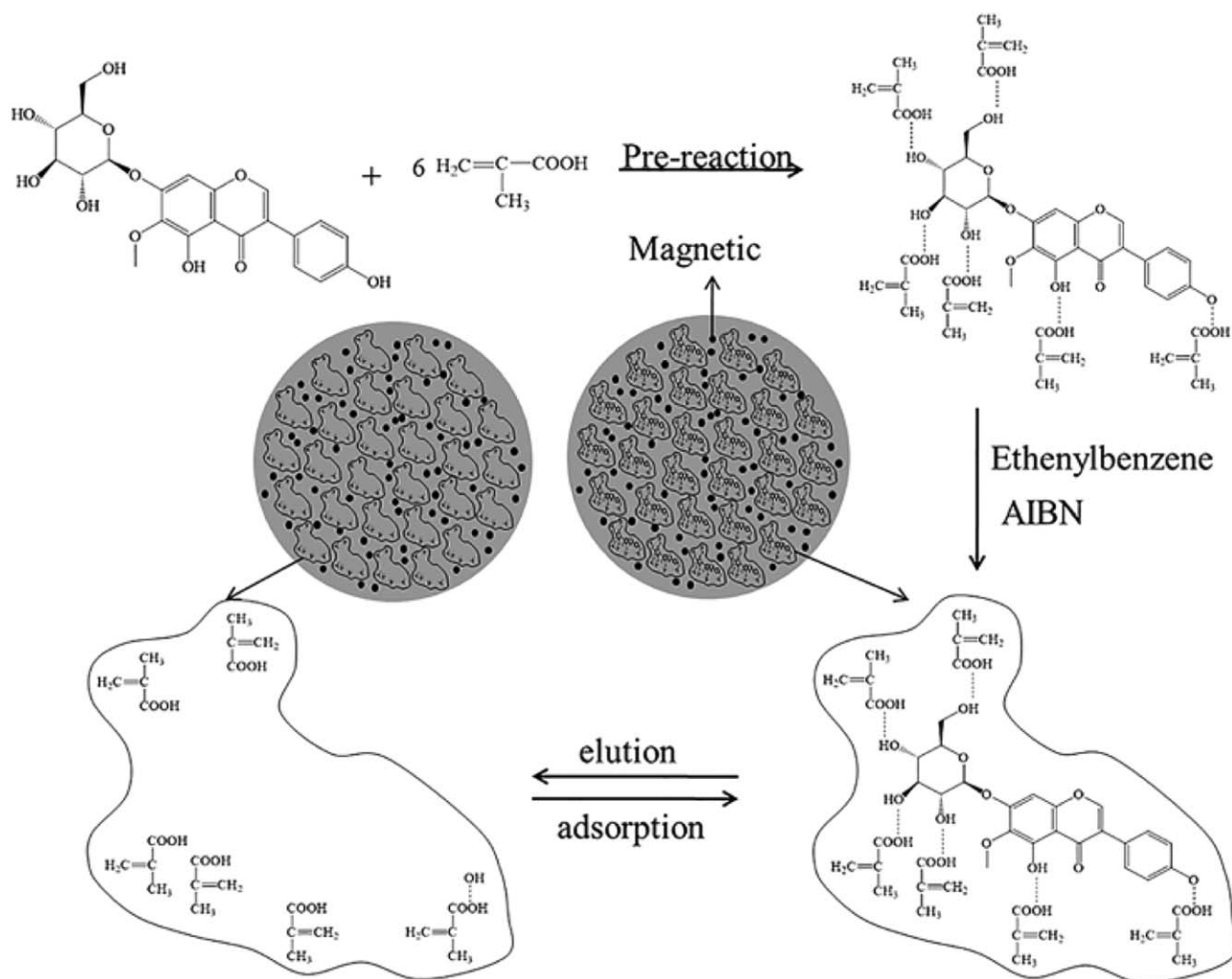


Figure 1. Schematic illustration for synthesis of TIMNPs.

$\text{Fe}_3\text{O}_4$  nanoparticles ( $2\theta = 30.24^\circ, 35.64^\circ, 43.35^\circ, 53.78^\circ, 57.34^\circ, 62.91^\circ$ ). The six discernible characteristic peaks could be indexed to (220), (311), (400), (422), (511), and (440), which match well with the database of magnetite in JCPDS (JCPDS Card: 19-629) file.<sup>39</sup> The results suggest that the  $\text{Fe}_3\text{O}_4$  nanoparticles and TIMNPs are of the same crystal structure.

The magnetic properties of the synthesized nanoparticles are of great interest for all further applications. Figure 6 shows the magnetic hysteresis loop analysis of  $\text{Fe}_3\text{O}_4$  nanoparticles (a) and TIMNPs (b), respectively. All of the nanoparticles show a typical superparamagnetic behavior at low field range. The saturation magnetization ( $M_s$ ) values obtained at room temperature are 75.88 and 29.84 emu/g for  $\text{Fe}_3\text{O}_4$  and TIMNPs, respectively. The loss of magnetization, on one hand, may be caused by the formation of some non-magnetic iron oxide ( $\text{Fe}_2\text{O}_3$ ) during the sonication progress. On the other hand, it may be because the containing of polystyrene reduces the  $M_s$  consequently. However, it is observed that TIMNPs could be attracted faster than the  $\text{Fe}_3\text{O}_4$  nanoparticles under the same external magnetic field. This trend infers that the content of  $\text{Fe}_3\text{O}_4$  in TIMNPs should be very high meanwhile the size of TIMNPs is much bigger than that of  $\text{Fe}_3\text{O}_4$  nanoparticles.<sup>40</sup>

In order to quantify the  $\text{Fe}_3\text{O}_4$  content in TIMNPs, the thermogravimetric analysis (TGA) was taken on  $\text{Fe}_3\text{O}_4$  nanoparticles (a), polystyrene microspheres (PS) (b), and TIMNPs (c). As shown in Figure 7, the mass loss of  $\text{Fe}_3\text{O}_4$  nanoparticles should be attributed to the crystal water in the samples. The weight loss of PS and TIMNPs between 370 and 450 °C are mainly due to the decomposition of polystyrene.<sup>41</sup> As shown in curve (b), it remains 3.05% impurities which cannot be ignored after polystyrene completely decomposed. The content of  $\text{Fe}_3\text{O}_4$  can be described as  $W\% = \frac{Wc\% - Wb\%}{Wa\% - Wb\%} \times 100\%$ , where  $Wa\%$ ,  $Wb\%$ , and  $Wc\%$  are the contents of decomposition remains of  $\text{Fe}_3\text{O}_4$  nanoparticles, PS, and TIMNPs, respectively. Therefore, the content of  $\text{Fe}_3\text{O}_4$  nanoparticles in TIMNPs is 46.87%. Due to the high content of magnetite, TIMNPs can be separated from an aqueous phase under an externally applied magnetic field quickly and completely.

#### Binding Properties and Scatchard Analysis of TIMNPs

As shown in Figure 8, TIMNPs have much higher recognition ability than the controlled NIMNPs. Scatchard analysis was used to discuss the binding properties for studying its specificity.<sup>42</sup>

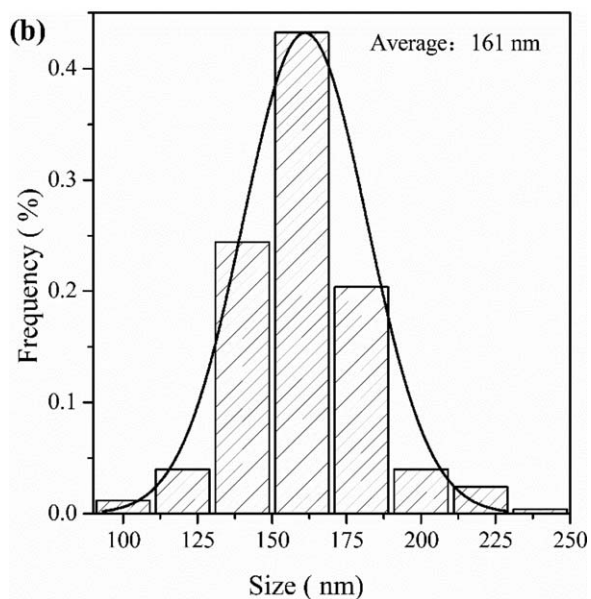
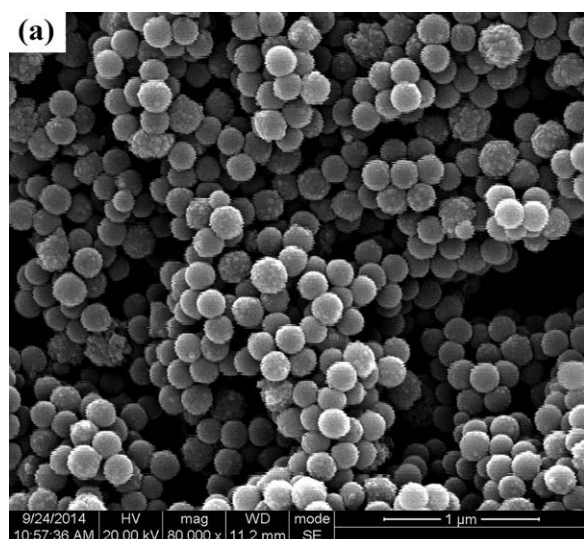


**Figure 2.** (a) SEM image of TIMNPs and (b) particle size distribution of TIMNPs.

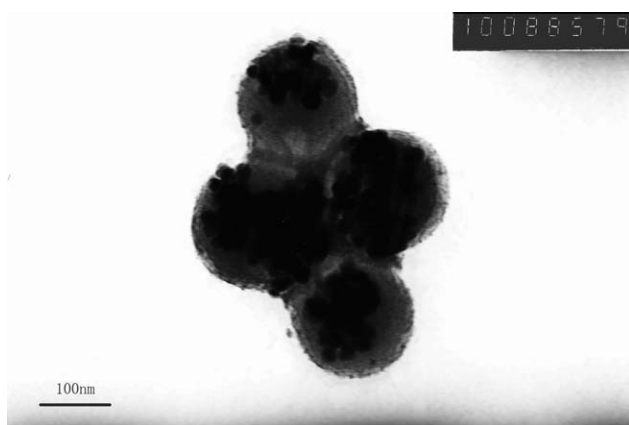


**Figure 3.** TEM image of TIMNPs.

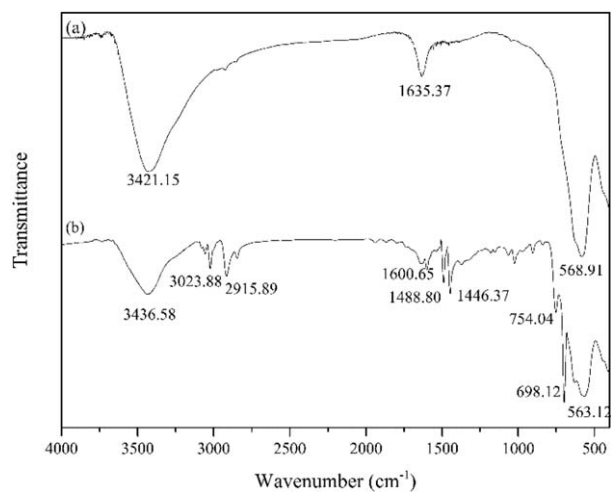


**Figure 4.** FTIR spectra of Fe<sub>3</sub>O<sub>4</sub> nanoparticles (a) and TIMNPs (b).

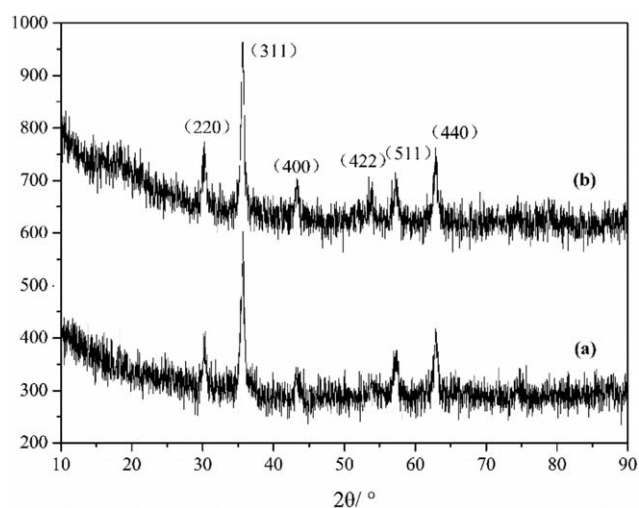


**Figure 5.** XRD spectra of Fe<sub>3</sub>O<sub>4</sub> nanoparticles (a) and TIMNPs (b).

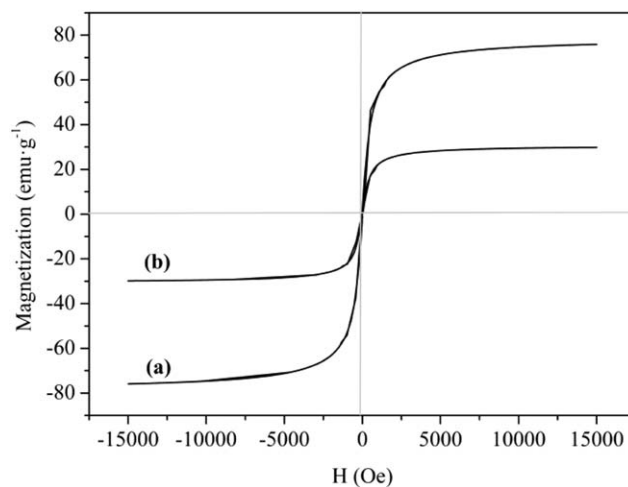


**Figure 6.** Magnetic hysteresis curves of Fe<sub>3</sub>O<sub>4</sub> nanoparticles (a) and TIMNPs (b).



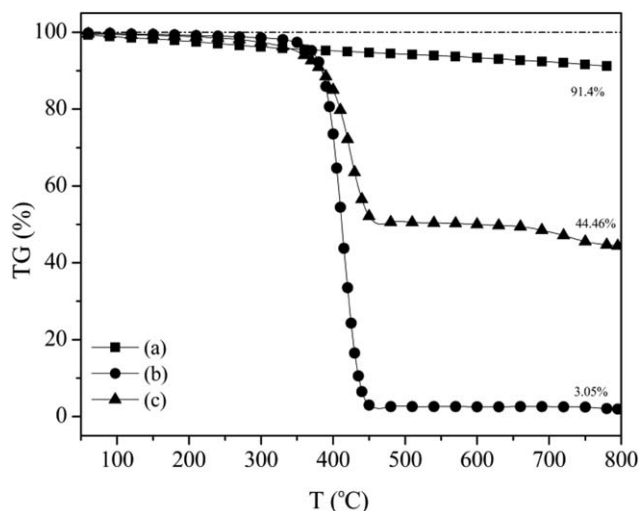


Figure 7. TGA curves of Fe<sub>3</sub>O<sub>4</sub> nanoparticles (a), PS (b), and TIMNPs (c).

The Scatchard equation is as follows:

$$\frac{Q}{C_e} = \frac{(Q_{\max} - Q)}{K_d} \quad (1)$$

where  $Q$  is the amount of tectoridin bound to TIMNPs at equilibrium,  $Q_{\max}$  is the apparent maximum number of binding sites,  $C_e$  is the free analytical concentration at equilibrium, and  $K_d$  is the dissociation constant. Scatchard graph (Figure 9) was plotted based on eq. (1) (inset of Figure 8). It is observed that the Scatchard plot is a single straight line, which indicates that there is only one kind of binding sites existed in the imprinted magnetic nanoparticles. The linear equation is:

$$\frac{Q}{C_e} = -0.833 Q + 57.959, (R_2 = 0.99389)$$

The value of  $K_d$  and  $Q_{\max}$  are 1.20 mol/L and 69.58  $\mu\text{mol/g}$ , respectively, which are calculated from the slopes and intercepts. The data indicated a good binding capacity comparing with the results of other published articles.<sup>43–45</sup>

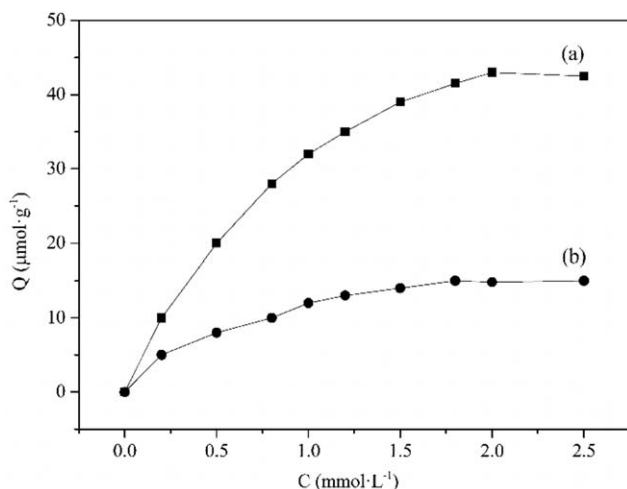


Figure 8. Binding isothermals of TIMNPs (a) and NIMNPs (b).

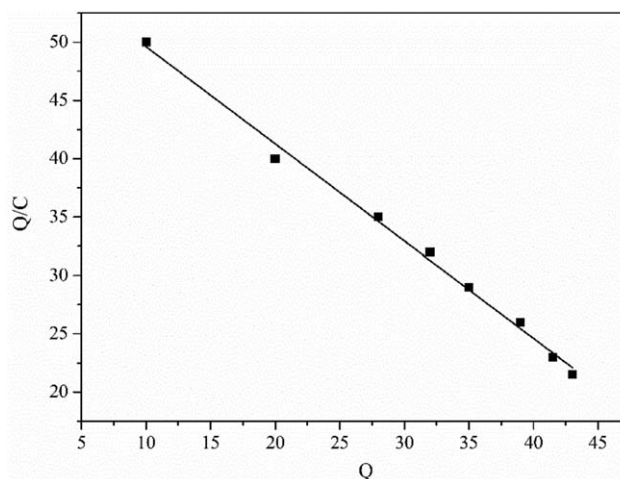


Figure 9. Scatchard plots to estimate the binding nature of TIMNPs.

### Adsorption Selectivity

The unique selective recognition of TIMNPs toward tectoridin was investigated by calculating adsorption amount of tectoridin

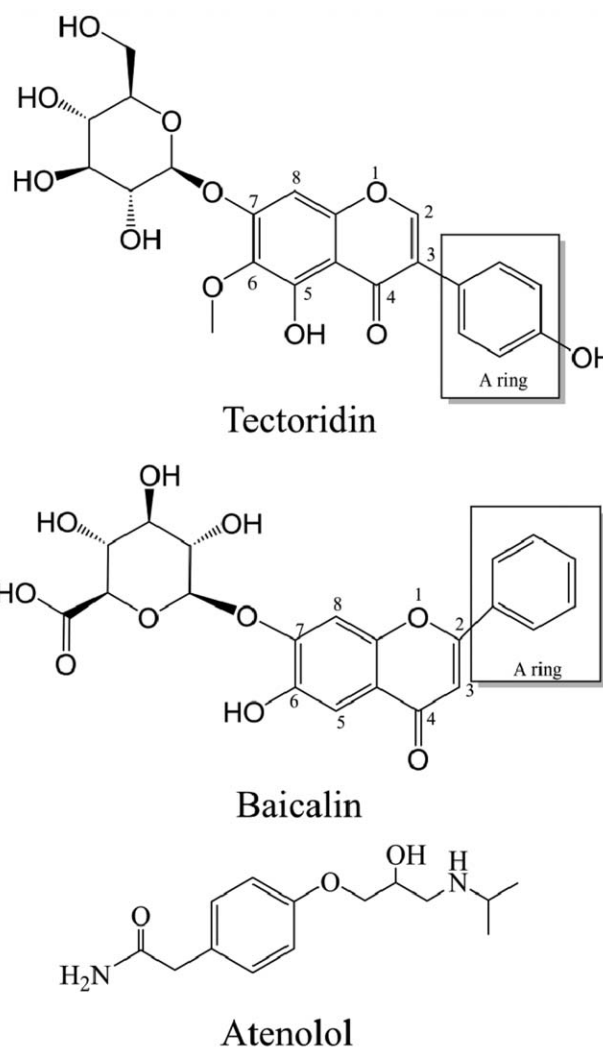


Figure 10. Molecular structures of tectoridin, baicalin, and atenolol.

structural analogues, such as baicalin, and non-structural analogues, such as atenolol (Figure 10). Tectoridin and baicalin all belong to flavonoid compounds. Tectoridin with parenting structure 3-phenyl-chromones is a kind of isoflavones, while baicalin is a kind of flavones with the parenting structure of 2-phenyl-chromones. The site of the A ring (benzene ring) is the most significant difference between isoflavones and flavones (shown in Figure 10). And the connected glucuronide are not the same. These differences between tectoridin and baicalin could be recognized by the TIMNPs. The molecular of atenolol is much smaller than that of tectoridin but it does not have enough hydroxyl groups to form hydrogen bonding with the recognition site. The adsorption selectivity experiments of the three compounds were taken under the same conditions and the results were shown in Figure 11.

Static distribution factor ( $K_d$ ), separation factor ( $\alpha$ ), and relative separation factor ( $\beta$ ) were used to evaluate the selectivity of TIMNPs. The equations are as follows:

$$K_d = \frac{C_p}{C_s} \quad (2)$$

$$\alpha = \frac{K_{d1}}{K_{d2}} \quad (3)$$

$$\beta = \frac{\alpha_1}{\alpha_2} \quad (4)$$

where,  $C_p$  and  $C_s$  represent the adsorbed concentration and the equilibrium concentration;  $K_{d1}$  is static distribution coefficients of tectoridin while  $K_{d2}$  is for baicalin or atenolol;  $\alpha$  indicates the molecular recognition selectivity for TIMNPs to templates. In general, the larger the value of  $\alpha$ , the better the recognition selectivity is. Generally,  $\alpha_1$  and  $\alpha_2$  are the separation factors of TIMNPs and NIMNPs, respectively.  $\beta$  is relative separation factor which shows the difference between imprinted polymers and non-imprinted polymers. The larger the value of  $\beta$ , the higher the molecular recognition selectivity is resulted from imprinting. The experimental data and parameters were summarized in Table I.

It is evident that the values of  $K_d$  and  $\alpha$  of TIMNPs for tectoridin are more excellent than that for baicalin and atenolol. And the val-

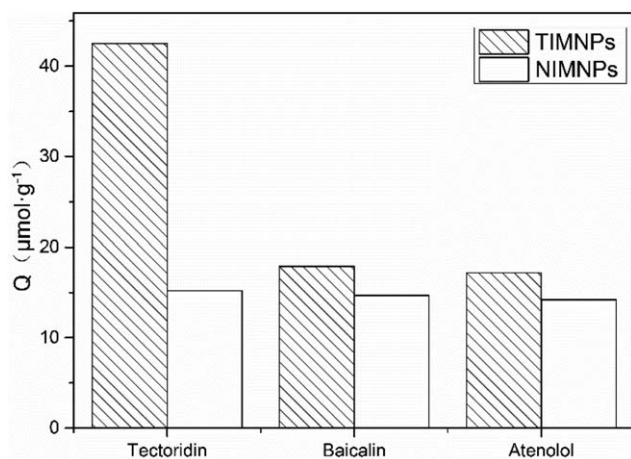


**Figure 11.** Adsorption selectivity of TIMNPs and NIMNPs for tectoridin, baicalin, and atenolol.

**Table I.** Separation Results of TIMNPs and NIMNPs from Tectoridin, Baicalin, and Atenolol

Molecular	$K_d$		$\alpha$		$\beta$
	TIMNPs	NIMNPs	TIMNPs	NIMNPs	
Tectoridin	26.98	8.23			
Baicalin	9.86	7.92	2.74	1.04	2.63
Atenolol	9.41	7.65	2.87	1.08	2.66

ues of NIMNPs for these compounds show less differentiation. The relative separation factors  $\beta$  are 2.63 and 2.66, respectively, indicating a good selectivity.<sup>46</sup> The results confirm clearly that TIMNPs have good specific recognition ability to the template tectoridin in comparison with structural analogue baicalin and non-structural analogue atenolol.

## CONCLUSIONS

In this work, we successfully synthesized TIMNPs by mini-emulsion polymerization for selective absorption of tectoridin. The prepared TIMNPs exhibited good binding capacity, absorption selectivity and saturation magnetization. It could be easily separated from the suspension by an external magnetic field, leading to a fast and selective recognition of tectoridin from aqueous solutions. All these results indicated that the synthesized TIMNPs could be one of the most promising candidates for tectoridin extraction.

## ACKNOWLEDGMENTS

This work is supported by National Natural Science Foundation of China (No. 20975072). The authors thank the Instrumental Analysis Center of Sichuan University for the characterizations of products.

## REFERENCES

- Dong, X. P.; Yang, Y. X. *Pharm. Clin. Chin. Mater. Med.* **2010**, *1*, 20.
- Zhan, R.; Jiao, Z. H.; Wang, H. L. *Gansu J. Tradit. Chin. Med.* **2011**, *24*, 78.
- Sun, Y. S.; Li, W.; Wang, J. H. *J. Chromatogr. B* **2011**, *879*, 975.
- Shin, J.; Bae, E.; Lee, Y. C.; Ma, J.; Kim, D. *Biol. Pharm. Bull.* **2006**, 1202.
- Lee, H.; Bae, E.; Kim, D. *J. Pharmacol. Sci.* **2005**, *97*, 541.
- Jung, S. H.; Lee, Y. S.; Lim, S. S.; Lee, S. H.; Shin, K. H.; Kim, Y. S. *Arch. Pharm. Res.* **2004**, *3*, 184.
- Park, J.; Park, E.; Kim, D.; Jung, K.; Jung, J.; Lee, E.; Hyun, J.; Kang, J. L.; Kim, H. *J. Neuroimmunol.* **2009**, *209*, 40.
- Fang, R.; Houghton, P. J.; Hylands, P. J. *J. Ethnopharmacol.* **2008**, *118*, 257.
- Duang, L. H.; Zheng, B. S.; Guo, S. Y. *J. Food Sci. Biotechnol.* **2009**, *1*, 44.
- Bai, L. Q.; Lou, J. S. *Acta Acad. Med. CPAF* **2008**, *10*, 837.

11. Liu, L. L.; Ma, Y. J.; Chen, X. Q.; Xiong, X.; Shi, S. Y. *J. Chromatogr. B* **2012**, 887-888, 55.
12. Ou, J. J.; Kong, L.; Pan, C. S.; Su, X. Y.; Lei, X. Y.; Zou, H. F. *J. Chromatogr. A* **2006**, 1117, 163.
13. Chen, L. G.; Zhang, X. P.; Xu, Y.; Du, X. B.; Sun, X.; Sun, L.; Wang, H.; Zhao, Q.; Yu, A. M.; Zhang, H. Q.; Ding, L. A. *Chim. Acta* **2010**, 662, 31.
14. Wang, X. J.; Xu, Z. L.; Feng, J. L.; Bing, N. C.; Yang, Z. G. *J. Membr. Sci.* **2008**, 313, 97.
15. Lenain, P.; Diana Di Mavungu, J.; Dubruel, P.; Robbens, J.; De Saeger, S. *Anal. Chem.* **2012**, 84, 10411.
16. Yamazaki, T.; Yilmaz, E.; Mosbach, K.; Sode, K. *Anal. Chim. Acta* **2001**, 435, 209.
17. Ye, L.; Mosbach, K. *J. Am. Chem. Soc.* **2001**, 123, 2901.
18. Prasad, B. B.; Srivastava, A.; Tiwari, M. P. *J. Colloid Interf. Sci.* **2013**, 396, 234.
19. Wulff, G. *Chem. Rev.* **2002**, 102, 1.
20. Brüggemann, O. *Anal. Chim. Acta* **2001**, 435, 197.
21. Brüggemann, O.; Haupt, K.; Ye, L.; Yilmaz, E.; Mosbach, K. *J. Chromatogr. A* **2000**, 889, 15.
22. Hirayama, K.; Sakai, Y.; Kameoka, K. *J. Appl. Polym. Sci.* **2001**, 3378.
23. Pérez-Moral, N.; Mayes, A. G. *Langmuir* **2004**, 20, 3775.
24. Carter, S. R.; Rimmer, S. *Adv. Funct. Mater.* **2004**, 14, 553.
25. Lu, C. H.; Zhou, W. H.; Han, B.; Yang, H. H.; Chen, X.; Wang, X. R. *Anal. Chem.* **2007**, 79, 5457.
26. Guo, T.; Deng, Q. L.; Fang, G. Z.; Liu, C. C.; Huang, X.; Wang, S. *Biosens. Bioelectron.* **2015**, 74, 498.
27. Sanagi, M. M.; Salleh, S.; Ibrahim, W. A. W.; Naim, A. A.; Hermawan, D.; Miskam, M.; Hussain, I.; Aboul-Enein, H. Y. *J. Food. Compos. Anal.* **2013**, 32, 155.
28. Niu, D. D.; Zhou, Z. P.; Yang, W. M.; Li, Y.; Xia, L.; Jiang, B.; Xu, W. Z.; Huang, W. H.; Zhu, T. Y. *J. Appl. Polym. Sci.* **2013**, 130, 2859.
29. Cutivet, A.; Schembri, C.; Kovensky, J.; Haupt, K. *J. Am. Chem. Soc.* **2009**, 131, 14699.
30. Sellergren, B. *Nat. Chem.* **2010**, 2, 7.
31. Abdin, M. J.; Altintas, Z.; Tothill, I. E. *Biosens. Bioelectron.* **2015**, 67, 177.
32. Ansell, R. J.; Mosbach, K. *Analyst* **1998**, 123, 1611.
33. Jing, T.; Du, H.; Dai, Q.; Xia, H.; Niu, J.; Hao, Q.; Mei, S.; Zhou, Y. *Biosens. Bioelectron.* **2010**, 26, 301.
34. Li, L.; He, X.; Chen, L.; Zhang, Y. *Chem. Asian J.* **2009**, 4, 286.
35. Wang, X.; Wang, L.; He, X.; Zhang, Y.; Chen, L. *Talanta* **2009**, 78, 327.
36. Wen, H.; Gao, G.; Han, Z.; Liu, F. *Polym. Int.* **2008**, 57, 584.
37. Ma, M.; Zhang, Y.; Yu, W.; Shen, H.; Zhang, H.; Gu, N. *Colloids Surf. A* **2003**, 212, 219.
38. Cui, L.; Xu, H.; He, P.; Sumitomo, K.; Yamaguchi, Y.; Gu, H. *J. Polym. Sci. Part A: Polym. Chem.* **2007**, 45, 5285.
39. Pan, J.; Xu, L.; Dai, J.; Li, X.; Hang, H.; Huo, P.; Li, C.; Yan, Y. *Chem. Eng. J.* **2011**, 174, 68.
40. Huang, Z.; Tang, F. *J. Colloid Interf. Sci.* **2004**, 275, 142.
41. Charoenmark, L.; Polpanich, D.; Thiramanas, R.; Tangboriboonrat, P. *Macromol. Res.* **2012**, 20, 590.
42. Chen, L.; Zhang, X.; Sun, L.; Xu, Y.; Zeng, Q.; Wang, H.; Xu, H.; Yu, A.; Zhang, H.; Ding, L. *J. Agric. Food. Chem.* **2009**, 57, 10073.
43. Wang, X.; Ding, X.; Zheng, Z.; Hu, X.; Cheng, X.; Peng, Y. *Macromol. Rapid Commun.* **2006**, 27, 1180.
44. Lin, Q.; He, J.; Liu, L.; Deng, Q. *Acta Sci. Nat. Univ. Sunyatseni* **2004**, 43, 51.
45. Zhu, H.; Wang, Y.; Yuan, Y.; Zeng, H. *Anal. Methods* **2011**, 3, 348.
46. Lu, S.; Cheng, G.; Zhang, H.; Pang, X. *J. Appl. Polym. Sci.* **2006**, 99, 3241.

SGML and CITI Use Only  
DO NOT PRINT

